Effect of Ultraviolet Light Irradiation on Gas Permeability in Polyimide Membranes. II. Irradiation of Membranes with High-Pressure Mercury Lamp

SHIGETOSHI MATSUI, TSUTOMU NAKAGAWA

Department of Industrial Chemistry, Meiji University, Kawasaki 214-71, Japan

Received 27 November 1996; accepted 6 June 1997

ABSTRACT: A photocrosslinkable polyimide membrane was prepared and investigated with regard to the effect of ultraviolet light irradiation (UV-irradiation) using a high-pressure mercury lamp on their gas permeabilities and permselectivities. Permeability and diffusion coefficients for O_2, N_2, H_2, and CO_2 were determined using the vacuum-pressure and time-lag methods. Sorption properties for carbon dioxide were determined to evaluate the changes in the free volume in the membranes by the irradiation. The apparent gas permeabilities decreased and permselectivity, particularly for H_2 over N_2, increased with increasing UV-irradiation time without a significant decrease in the flux of H_2. They depended on the membrane thickness, suggesting asymmetrical changes in the membrane due to UV-irradiation. © 1998 John Wiley & Sons, Inc. J Appl Polym Sci **67:** 49–60, 1998

Key words: polyimide membrane; ultraviolet light irradiation; crosslinking; densification; gas permeability

INTRODUCTION

Aromatic polyimides have been extensively studied in various manufacturing fields because of their excellent properties, e.g., thermal stability, chemical resistance, mechanical strength, and low dielectric constant. In the field of polymeric membranes for gas-separation applications, polyimide membranes were studied because of the diversity of their structures and their high gas selectivities.[1–6] On the other hand, their permeabilities are relatively low compared to the other nonporous polymeric membranes and few polyimide membranes overcome the trade-off relationship between gas permeability and selectivity. Many investigators have made efforts to create or improve the membranes not limited to the polyimide membranes in order to overcome this relationship. In the improvements of the gas selectivities in the polyimide membranes, investigations of the UV-irradiation on the membranes to introduce crosslinking into them, which causes effective reduction of the diffusivities of the large gas molecules such as N_2 and CO_2, resulting in the increasing permselectivities for the large–small gas pairs, were conducted.[7–9] Thus, Hayes reported the effect of UV-irradiation on the gas permeabilities and selectivities in photocrosslinkable polyimide membranes which contain the benzophenone structure and alkyl side chains.[7] The author concluded that this was due to the optimization of the free volume, through which the gas molecules permeate, by chemical crosslinking. Kita et al.[8] and Xu et al.[9] also used similar polyimide membranes as in the above research. Moreover, we previously reported (Part I) the effect of UV-irradiation with a low-pressure mercury lamp on the gas permeability in the benzophenone type and noncrosslinkable-type polyimide membranes as

Correspondence to: T. Nakagawa.

Journal of Applied Polymer Science, Vol. 67, 49–60 (1998)
 CCC 0021-8995/98/010049-12

one of the efficient improvements of their gas selectivity, i.e., increasing their gas selectivity in maintaining the higher flux gases such as H_2.[10] We also showed the physical changes as well as chemical changes of polyimide membranes by UV-irradiation in the previous article. As a result of previous work, the changes in the gas-permeation properties of polyimide membranes which were crosslinkable and noncrosslinkable by UV-irradiation were due to physical densification of the membranes.

In this work, Part II, a high-pressure mercury lamp was utilized as a UV source while a low-pressure mercury lamp was used in the previous article. We studied the effect of UV-irradiation using a high-pressure mercury lamp on the gas permeabilities and gas selectivities in the polyimide membranes having a benzophenone structure by varying the irradiation procedure and condition of the membrane before irradiation. Moreover, a detailed investigation of the thickness dependence of the gas permeability was newly made. This result also brought insight into the morphological change in the membrane due to UV-irradiation.

THEORETICAL BACKGROUND

Gas Permeation and Sorption

The permeability coefficient, P, for the penetrant molecules in the nonporous polymeric membrane can be written as follows using the diffusivity coefficient, D, and solubility coefficient, S[11]:

$$P = D \cdot S \tag{1}$$

This equation should be applied to the noninteractive polymer–penetrant systems. In the case of the permeation of carbon dioxide or hydrocarbons through a glassy polymer like polyimide, the solubility and diffusion coefficients depend on the penetrant concentration. The permeability coefficient also depends on it. However, if the concentration is low enough, it can be regarded as a constant. For the glassy polymers, these coefficients as well as the permeability coefficient are apparent values.

The permeability and diffusion coefficients were experimentally calculated from the steady-state slope of the pressure–time curve and the membrane thickness. The permeation rate, P_R, and permeability coefficient, P, are determined using the following equations:

$$P_R = (dp/dt) \cdot (273 \cdot V/760 \cdot K)/(A \cdot p_1) \tag{2}$$

$$P = P_R \cdot l \tag{3}$$

where dp/dt is the increment of pressure per unit time on the gas permeate side; V, the volume of the permeate side; K, the absolute temperature; and A, the effective area of the membrane. The pressure at the permeate side is ignored in eq. (2).

The diffusion coefficient was calculated with the time lag, θ, from the following equation[11]:

$$D = l^2/6\theta \tag{4}$$

Dividing the permeability coefficient by the experimentally determined diffusion coefficient gives the solubility coefficient using eq. (1).

Based on the temperature dependence of the permeability and diffusion coefficients, activation energies can be determined using the Arrhenius equation[11]:

$$P = P_0 \exp(-E_P/RT) \tag{5}$$

$$D = D_0 \exp(-E_D/RT) \tag{6}$$

where E_P and E_D are the apparent activation energies for permeation and diffusion, respectively; P_0 and D_0 are preexponential factors; and R is the gas constant. These activation energies are indications for the ease of the permeation or diffusion of the gas molecules through the membrane. The solubility, also described by the heat of solution, ΔH_S, is described as follows:

$$S = S_0 \exp(-\Delta H_S/RT) \tag{7}$$

where S_0 is also the preexponential factor. The following equation can be derived from eqs. (1) and (5)–(7):

$$E_P = E_D + \Delta H_S \tag{8}$$

As shown later, the polyimide membrane used in this work became asymmetric in the direction of the gas permeation by UV-irradiation. According to the multilayer permeation theory,[12] the gas permeation through binary layers is described as follows if the layer that is affected by UV-irradiation is simply homogeneous for the gas permeation:

$$l_{1,2}/P_{1,2} = l_1/P_1 + l_2/P_2 \tag{9}$$

where P and l are the permeability coefficients and the thickness of the layer, respectively, as mentioned previously and the subscripts are the number of layers.

The ideal separation factor through the membrane is calculated with the permeability coefficients for components A and B or the permeation rates:

$$\alpha_{A/B} = P_A/P_B = Q_A/Q_B \quad (10)$$

Based on the dual-mode sorption model,[13,14] the sorption isotherm, which can give the solubility coefficient at the equilibrium state under a certain pressure, for the carbon dioxide in the glassy polymer is described as follows:

$$C = C_D + C_H = k_D p + C'_H bp/(1 + bp) \quad (11)$$

where C is the gas concentration in the polymer and subscripts D and H indicate the dissolution by the Henry's law mechanism and sorption into the microvoid by the Langmuir mechanism, respectively. The parameter k_D is the solubility coefficient of the Henry's law; C'_H, the capacity; and b, the hole affinity constant of Langmuir sorption. These parameters are mostly used to estimate the gas-permeation properties of the glassy polymer membranes. They are changed by the various treatments, e.g., thermal treatment[15,16] and exposure to the gas plasticizing the polymers,[17–19] which result in changes in the permeation properties. In other words, these parameter changes give us insight into the morphological changes in the bulk membrane.

Depth Profiling Using ATR Method

The attenuated total reflection (ATR) spectrum reflects the average surface structure of the material for a limited depth. In organic compounds, this detectable depth mainly depends on the material selected as an internal reflection element (IRE), the incident angle, and the observed wavelength and is described as follows[20,21]:

$$d_p = \lambda/2\pi n_1\{\sin^2\theta - (n_2/n_1)^2\}^{1/2} \quad (12)$$

where d_p is the detectable depth from the surface; λ, the wavelength; θ, the incident angle, and n_1 and n_2, the refractive indices of the IRE and the sample, respectively. In general, refractive indices of organic compounds are about 1.5; and for the germanium crystal, it is 4.0.

EXPERIMENTAL

Polymer Preparation

The monomers used in this study, 3,3′,4,4′-benzophenonetetracarboxylic dianhydride (BTDA) and 2,2-bis[4-(4-aminophenoxy)phenyl]-propane (BAPP), were obtained from Tokyo Kasei Kogyo Co. Dianhydrides and diamines were recrystallized with acetic anhydride and 2-propanol, respectively. The solvent, *N,N*-dimethylformamide (DMF), was dehydrated with well-dried molecular sieves.

Polyimide membranes, BTDA–BAPP, were prepared by the same procedure described in the previous article.[10] The polyimide membrane used in this study was moderately cooled (BTDA–BAPP) or quenched [BTDA–BAPP(Q)] to room temperature after the thermal imidization. The schematic representation of the preparation and chemical structures of the polyimide as well as the monomers are shown in Figure 1.

The polyimide membrane was exposed to a high-pressure mercury lamp (400 W, Sen Light Corp.) in the air at a distance of 10 cm. The temperature and UV intensity at the surface of the membrane, which was irradiated in the air, was about 50°C and 10.3 mW/cm^3, respectively.

Polymer Characterization

The FTIR spectrum of the membrane was obtained using the ATR method with the germanium crystal or KRS-5 as an IRE at incident angles of 30°, 45°, and 60° for the germanium and 45° for KRS-5 using a Perkin-Elmer 1800. Wide-angle X-ray diffraction was performed on a Rigaku RINT 1200 utilizing CuKα (λ = 1.54 Å) radiation. The specific gravity was determined using a calcium nitrate aqueous solution at room temperature. The glass transition temperature (T_g) was determined using a Perkin-Elmer DSC-7 at a heating rate of 20°C. The degree of imidization of the membrane was estimated by thermogravimetry (TG) and FTIR.

Gas-Permeation and -Sorption Properties

To determine the gas-permeation properties of the membranes, the vacuum-pressure and time-lag

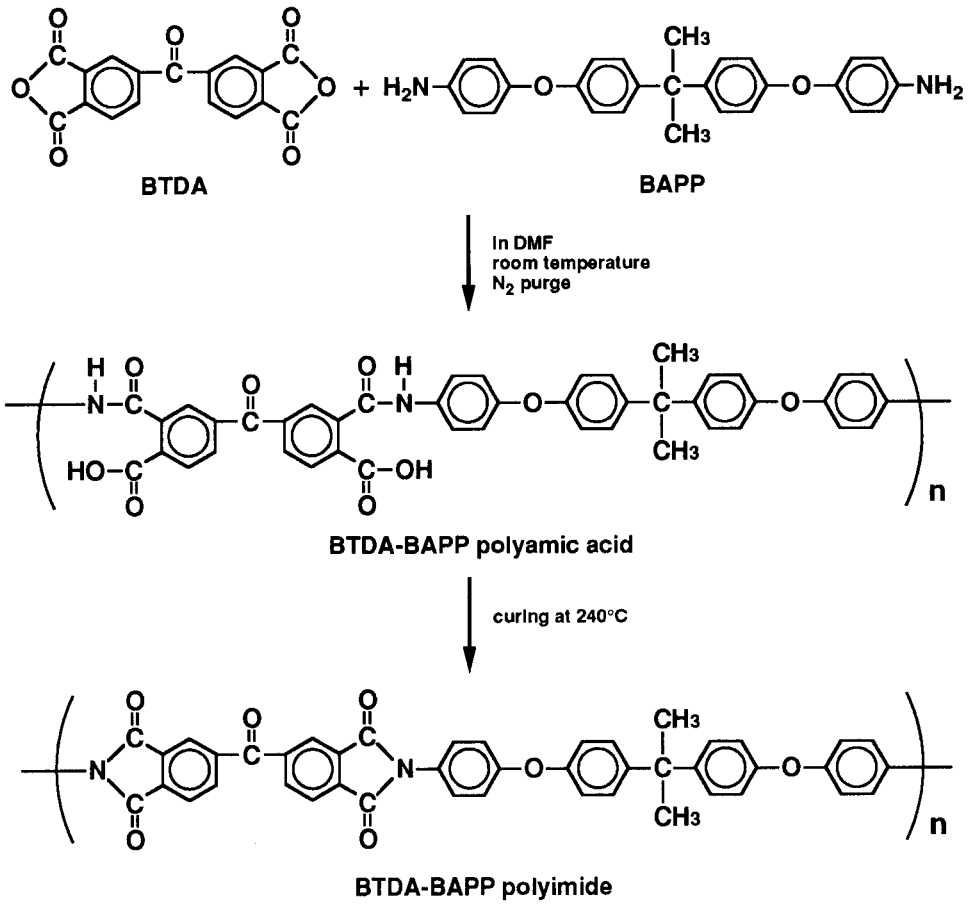

Figure 1 Schematic representation of the preparation and chemical structures of the polyimide and monomers studied.

methods were employed. The apparatus for the gas-permeation measurement was schematically described and its method was reported elsewhere.[22] The gas-permeation measurements were carried out for pure H_2, N_2, O_2, and CO_2 in the range of ambient temperature to 100°C. These gases were supplied by Showa Denko Co. and used without further purification.

The gas-sorption properties of the polyimide membranes for carbon dioxide were determined by the gravimetric method. The apparatus and procedure for this measurement were described previously.[10]

RESULTS AND DISCUSSION

Polymer Characterization

Polymerization and Solubility for Solvent of Polyimides

Because the bands attributed to the amide moiety and carboxyl group in the amide bond were not observed in the thermally imidized membranes in the FTIR spectra and the dehydration between a carboxylic acid and an amine was not observed in the TG curves, the degree of imidization of the membranes was more than 95%. Even after irradiation, a decrease in these values was not observed in the bulk membrane from the DSC curves or also at the surface of the membrane from the ATR spectra. The T_g of the polyimide membrane was about 234°C.

ATR Analysis of UV-Irradiated Polyimides

The ATR spectra of the BTDA–BAPP and UV-irradiated BTDA–BAPP membranes in the range of 700–4000 cm^{-1} are shown in Figure 2. In these spectra, the 1360, 1730, and 1780 cm^{-1} bands are attributed to the imide moiety. The 1680 cm^{-1} band is attributed to the carbonyl group in the benzophenone structure. The intensity of this 1680 cm^{-1} band decreased with increasing UV-irradiation time in the BTDA–BAPP membrane.

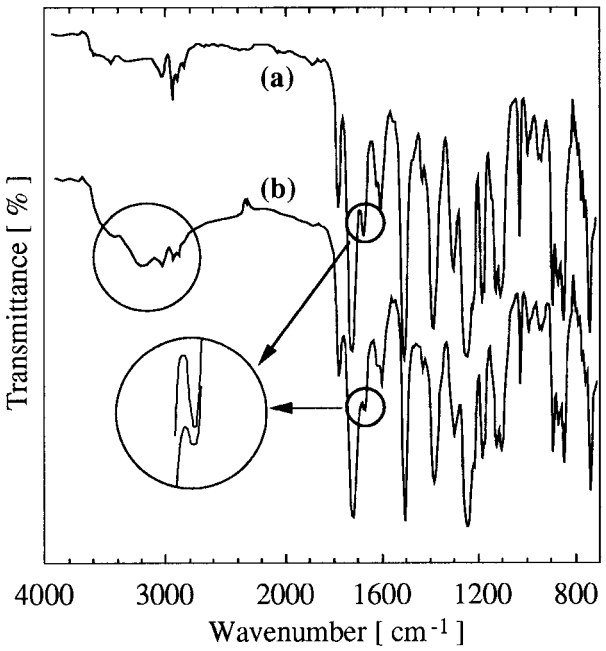

Figure 2 FTIR-ATR spectra of the (a) BTDA–BAPP and (b) BTDA–BAPP irradiated for 30 min.

On the other hand, the intensity of the band around 3500 cm^{-1}, which is attributed to the hydroxyl group formed by hydrogen abstraction or the oxidation, was increased by the irradiation.

The polyimide having the benzophenone structure and alkyl side chains, in both the liquid and solid states, was crosslinked by UV-irradiation via the following mechanism[23]: (1) excitation of the carbonyl group in the benzophenone by UV-irradiation, resulting in the ketyl radicals; (2) hydrogen abstraction by the ketyl radicals from the alkyl groups, resulting in the alkyl radicals; and (3) binding between these radicals. The carbonyl groups in the benzophenone are chemically changed by the UV-irradiation. Therefore, their absorption bands in the infrared spectrum decreased.

Figure 3 shows the depth profiling of the carbonyl group at 1680 cm^{-1} in the benzophenone structure in the BTDA–BAPP membrane. It is assumed here that the absorbance of the benzene ring at about 1500 cm^{-1} are not changed by UV-irradiation. The ratio, A_{1680}/A_{1500}, in the nontreated BTDA–BAPP is normalized to unity. The relative intensities of A_{1680}/A_{1500} in the UV-irradiated BTDA–BAPP membranes to that in the nontreated one are then plotted at the four-depth calculated from eq. (11) in this figure. The relative intensities decreased as the incident angle increased, i.e., the nearer to the surface of the irradiated side of these carbonyl groups, the more they were chemically changed by the irradiation. These intensities as well as the other band's intensities on the opposite side of the irradiated side of the membranes were not changed by UV-irradiation, indicating that the chemical changes occurred only at the UV-irradiated side of the membrane and hence, that the membrane became inhomogeneous for the gas-permeation properties.

As it could not be judged by the ATR method that the BTDA–BAPP polyimide membrane was crosslinked by the irradiation, the effect of the crosslinking on the swelling of the membrane with the *N*-methyl-2-pyrrorydone was investigated. All the nontreated and irradiated BTDA–BAPP membranes similarly swelled about 30.0 $\pm$ 0.5 wt % at equilibrium. So, the differences due to irradiation could not be evaluated. Using the ultrathin BTDA–BAPP membrane, of which both sides were irradiated, for the above test, the solvent turned yellow, which was the polyimide color, in the nontreated membrane. On the other hand, in the irradiated membrane, the solvent remained almost colorless. This might be due to the formation of crosslinking in the BTDA–BAPP polyimide by UV-irradiation.

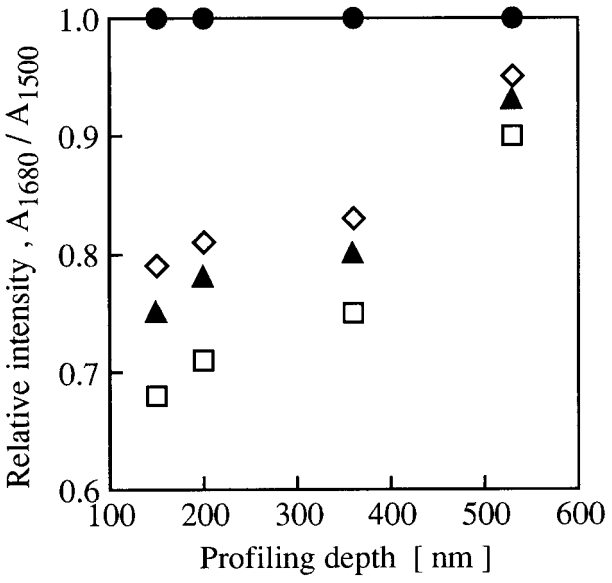

Figure 3 Variation in the relative intensities (normalized A_{1680}/A_{1500}) of the UV-irradiated BTDA–BAPP membranes compared with that of the nontreated membrane and their depth profiles: (●) nontreated; (◇) UV-irradiated for 10 min.; (▲) 20 min; (□) 30 min.

Table I Characterization of the Polyimide Membranes Studied

Membrane	Irradiation Time (min)	Specific Gravity (−)	*d*-Spacing (Å)
BTDA–BAPP	0	1.288	5.3
	10	1.289	5.2
	20	1.290	5.2
	30	1.291	5.2
BTDA–BAPP(Q)	0	1.286	5.4
	10	1.288	5.3
	20	1.289	5.3
	30	1.289	5.2

d-*Spacing and Specific Gravity of the Polyimides*

Various properties of the BTDA–BAPP and UV-irradiated membranes are shown in Table I. The mean interchain spacing of the polymer, the *d*-spacing, determined by WAXD, decreased slightly and specific gravities increased slightly with increasing UV-irradiation time. This suggests that UV-irradiation made the polyimide membrane slightly dense.

Effect of UV-Irradiation on Gas-Transport Properties

Permeabilities, Diffusivities, and Permselectivities

Stepwise Irradiated Membrane. The relationship between the total UV-irradiation time and the apparent gas permeability coefficients for O_2, N_2, H_2, and CO_2 in the BTDA–BAPP membrane, which was moderately cooled to room temperature after imidization, when the same membrane was stepwise irradiated for even 10 min, is shown in Figure 4. The apparent permeability coefficients for all gases studied decreased with total UV-irradiation time. These decreases were notable in the comparatively large gas molecules such as CO_2 and N_2. The apparent diffusion and solubility coefficients as well as permeability coefficients in this membrane are listed in Table II. Although these are apparent values because the membrane seems to have become asymmetric, which will be mentioned concerning the permeation properties in the membrane which was continuously irradiated, we can compare these values to one another because of using the same membrane to observe the effect of the irradiation. The diffusion coefficients decreased with the irradiation as seen in this Table I. This was due to the densification of the membrane by UV-irradiation. These are suspected from the effective decreases in the permeabilities for larger gas molecules such as CO_2 and N_2 by the irradiation. In fact, as shown in Figure 5, the larger the kinetic diameter determined from the Lennard-Jones force constants,[24] the more affected by the irradiation are the apparent diffusion coefficients, which increased in the diffusivity selectivities and resulted in the increase in the permselectivity. These are also suggested by the later discussion regarding the activation energy of diffusion. Moreover, the tendency to densification of the membranes due to the irradiation was found in their specific gravity and *d*-spacing although the changes in these values were not significant.

On the other hand, although the solubility coefficients were less comparable to one another because these were calculated with P and D using eq. (1), there are fewer effects of the irradiation on these values than on those on the diffusivities. In the solubility coefficients for the CO_2, which has a relatively high solubility for the glassy polymers, determined from the equilibrium sorption properties below 1 atm, small changes in these values were observed. From these results in the stepwise irradiated membrane, it seems that similar effects should follow in the successively irradiated membranes.

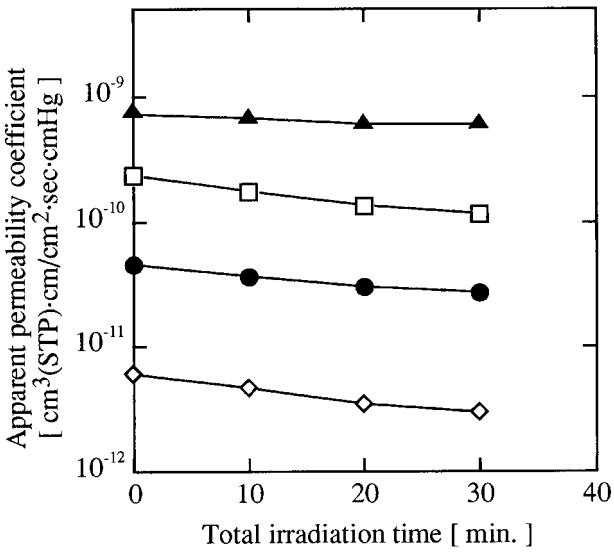

Figure 4 Relationship between the total UV-irradiation time and the apparent gas permeability coefficients for (●) O_2, (◇) N_2, (▲) H_2, and (□) CO_2 in the BTDA–BAPP membrane at 30°C.

Table II Apparent Permeation Properties for the Gases Studied in the Stepwise UV-Irradiated BTDA–BAPP Membranes at 30°C

Total Irradiation Time (min)	$P_{app.}$[a]				$D_{app.}$[b]			$S_{app.}$[c]			
	O_2	N_2	H_2	CO_2	O_2	N_2	CO_2	O_2	N_2	CO_2	PH_2/PN_2
0	0.45	0.060	7.7	2.3	0.96	0.19	0.17	4.7	3.1	138	130
10	0.36	0.046	7.0	1.8	0.75	0.14	0.12	4.8	3.4	144	152
20	0.30	0.034	6.3	1.4	0.67	0.11	0.098	4.4	3.1	140	183
30	0.27	0.029	6.3	1.2	0.61	0.10	0.086	4.5	2.9	135	215

[a] Apparent permeability coefficient $\times 10^{10}$ [cm^3 (STP) cm/cm^2 s cmHg].
[b] Apparent diffusion coefficient $\times 10^8$ (cm^2/s).
[c] Apparent solubility coefficient $\times 10^3$ [cm^{-3} (STP)/cm^3 (polymer) cmHg].

Successively Irradiated Membrane. The temperature dependence of the apparent permeability coefficients for O_2, N_2, H_2, and CO_2 in the BTDA–BAPP membrane is shown in Figure 6. The apparent permeability, diffusion, and solubility coefficients as well as the permeation rates for these gases in the BTDA–BAPP membrane are shown in Table III. Moreover, those of the BTDA–BAPP(Q) membrane and those of their successively UV-irradiated membranes at 30°C are also listed. Between the stepwise irradiation and the successive irradiation, the latter was more effective for the gas-permeation properties than was the former. These values of the UV-irradiated membranes are also apparent values as mentioned above and cannot be simply compared with each other because the membranes have become inhomogeneous in the direction of the permeation of the penetrants by the irradiation, which will be discussed later, and the membrane thicknesses are different from one another, but can be utilized for a qualitative comparison. The permeability coefficients for all the gases in the BTDA–BAPP membrane decreased with UV-irradiation time as expected from the results for the stepwise irradiated membrane. Comparing these permeation rates with one another instead of the permeability coefficients because the permeability coefficients

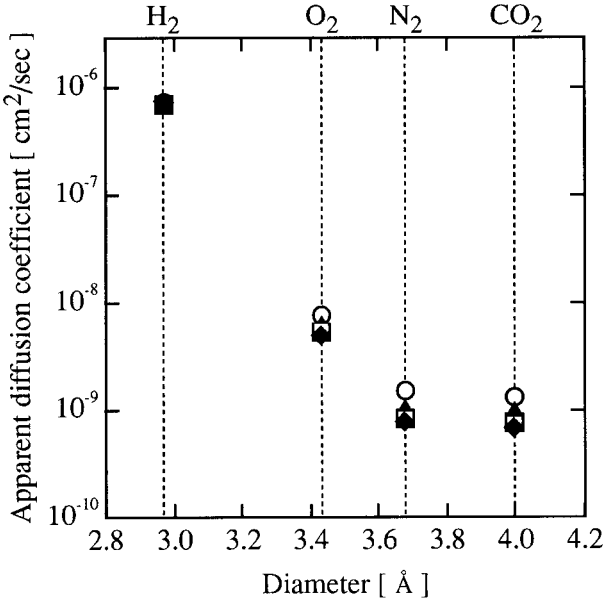

Figure 5 Relationship between the apparent gas diffusion coefficients in the stepwise UV-irradiated BTDA–BAPP membranes at 30°C and the kinetic diameter of the gas molecules: (○) nonirradiated; irradiated for (▲) 10 min, (□) 20 min, and (♦) 30 min.

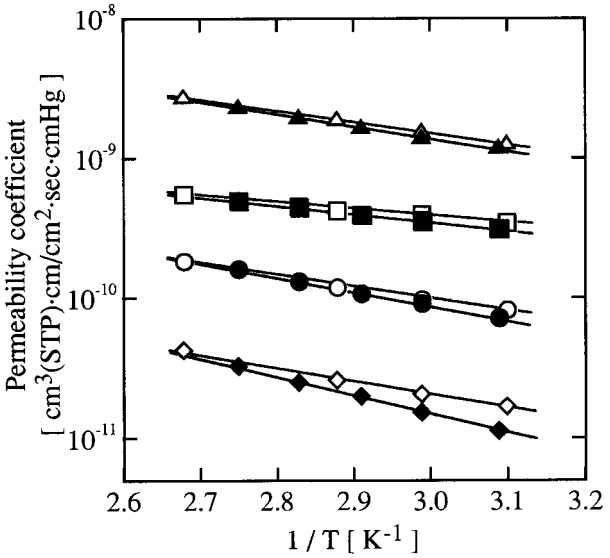

Figure 6 Temperature dependence of the apparent permeability coefficients for (○, ●) O_2, (◇, ♦) N_2, (△, ▲) H_2, and (□, ■) CO_2 gases in the (filled) BTDA–BAPP and (open) BTDA–BAPP(Q) membranes.

Table III Apparent Permeation Properties for the Gases Studied in the Successively UV-Irradiated BTDA–BAPP and BTDA–BAPP(Q) Membranes at 30°C

Membrane	Irradiation Time (min)	l[a] (μm)	$P_{app.}$[b]				PH_2/PN_2	$D_{app.}$[c]			$S_{app.}$[d]			P_R			
			O_2	N_2	H_2	CO_2		O_2	N_2	CO_2	O_2	N_2	CO_2	O_2	N_2	H_2	CO_2
BTDA–BAPP	0	48	0.45	0.060	7.7	2.3	130	0.96	0.19	0.17	4.7	3.1	138	0.93	0.12	16	4.9
	10	43	0.36	0.046	7.0	1.8	152	0.75	0.14	0.12	4.8	3.4	144	0.83	0.11	16	4.1
	20	56	0.36	0.043	7.1	1.8	164	0.71	0.13	0.11	5.1	3.5	168	0.65	0.077	13	3.1
	30	48	0.24	0.023	6.0	0.97	266	0.50	0.079	0.063	4.8	2.7	155	0.49	0.047	12	2.0
BTDA–BAPP(Q)	0	38	0.54	0.11	8.9	2.8	83	1.4	0.48	0.23	4.0	2.2	121	1.4	0.28	23	7.2
	10	51	0.47	0.064	8.5	2.4	132	1.0	0.18	0.17	4.6	3.5	147	0.91	0.13	17	4.8
	30	48	0.34	0.040	7.3	1.5	181	0.69	0.11	0.094	5.1	3.7	164	0.72	0.084	15	3.2

[a] Membrane thickness.
[b] Apparent permeability coefficient $\times 10^{10}$ [cm^3 (STP) cm/cm^2 s cmHg].
[c] Apparent diffusion coefficient $\times 10^8$ (cm^2/s).
[d] Apparent solubility coefficient $\times 10^3$ [cm^3 (STP)/cm^3 (polymer) cmHg].
[e] Permeation rate $\times 10^8$ [cm^3 (STP)/cm^2 s cmHg].

include the membrane thicknesses in their values, the permeation rates also decreased with the irradiation time in spite of even a decrease in the membrane thicknesses in the BTDA–BAPP membranes (e.g., comparing those of the nonirradiated membrane and one irradiated for 10 min). Theoretically, the permeation rate increases with decreasing thickness in the homogeneous membranes. These decreases in the successively irradiated membranes were due to the densification as were those of the stepwise irradiation. In fact, the membranes were slightly densified by the irradiation as shown in Table II. Furthermore, the apparent diffusion coefficients notably decreased, similar to the apparent permeability coefficients.

Effect of Cooling Processes After Thermal Imidization. The permeation properties for the gases studied in the BTDA–BAPP(Q) are listed in Table III. In the nonirradiated membranes, the permeability coefficients for all gases in the former were higher than those of the latter. This was consistent with other literature,[15] i.e., quenching to room temperature after the curing makes the unrelaxed free volume in the amorphous glassy polymers large. Basically, the decrease in the apparent gas permeability coefficients by the irradiation in this quenched membrane were similar to those of the moderately cooled BTDA–BAPP membrane. In terms of the permselectivity, that of the latter was larger than that of the former. These decreases in the permeabilities are also due to the densification of the membrane by the irradiation. However, especially in the BTDA–BAPP(Q) membrane irradiated for 10 min, a decrease in the unrelaxed free volume was observed with the sorption property for the carbon dioxide differing from that of the moderately cooled BTDA–BAPP membrane, as discussed in a later section.

Activation Energies and Heat of Sorption

The activation energies and heat of solution for the gases studied in the moderately cooled BTDA–BAPP membrane, which were calculated using the Arrhenius eqs. (5), (6), and (7), are listed in Table IV along with those of the UV-irradiated membranes. These are also apparent values because these are determined using the apparent values of the permeation properties. The activation energies of permeation, E_P, increased with the irradiation time. These are due to increases in the activation energies of the diffusion, E_D, because these changes were analogous to

Table IV Apparent Activation Energies of the Permeation and Diffusion and Heats of Solution for the Gases Studied in the UV-Irradiated BTDA–BAPP and BTDA–BAPP(Q) Membranes

Membrane	Irradiation Time (min)	$\bar{E}_P$[a]				$\bar{E}_D$[b]			$\Delta\bar{H}_S$[c]		
		O_2	N_2	H_2	CO_2	O_2	N_2	CO_2	O_2	N_2	CO_2
BTDA–BAPP	0	4.5	6.0	3.9	2.7	8.3	9.8	9.8	−3.8	−3.8	−7.1
	10	4.6	6.3	3.8	3.0	8.5	10	10	−3.9	−3.9	−7.2
	20	4.9	6.8	4.0	3.4	8.8	10	11	−3.8	−3.6	−7.4
	30	5.7	8.3	4.1	4.5	9.2	11	12	−3.5	−2.9	−7.1

[a] Apparent activation energy for the permeation (kcal/mol).
[b] Apparent activation energy for the diffusion (kcal/mol).
[c] Apparent heat of sorption (kcal/mol).

those of diffusion. Before the irradiation, the E_P of CO_2 was smaller than that of H_2. As seen in eq. (8), E_P is given by adding E_D to ΔH_S. When the exothermic heat of CO_2 sorption, $-\Delta H_S$, is relatively large with respect to the E_D of CO_2 compared with that of H_2 to its E_D, the E_P of CO_2 is smaller than that of H_2. After 30 min irradiation, however, the E_P of CO_2 was smaller than that of H_2. This was due to the drastic increase in E_D of CO_2 while the ΔH_S of CO_2 and the E_P of H_2 varied little.

The activation energies for the diffusion are also described as follows[25]:

$$E_D = 0.25 N_0 \pi d^2 \lambda \cdot (\mathrm{CED}) \qquad (13)$$

$$(\mathrm{CED}) = E_{\mathrm{coh}}/V_{\mathrm{mol}} \qquad (14)$$

where N_0 is Avogadro's number; d and λ, the diameter and length of a cylinder, respectively, formed when a diffusing molecule passes in the polymer matrix; CED, the cohesive energy density of the polymer; E_{coh}, the cohesive energy of the polymer; and V_{mol}, the molar volume of the polymer. According to eq. (13), the activation energy for the diffusion increases with increasing CED, d, or λ and is more sensitive to the diameter of the cylinder. These values are treated as constant and the activation energy is also a constant in a polymer as used for the calculation. Actually, they should be different for the various conditions of a polymer and a penetrant. Although d is the diameter of the gas molecule or of a cylinder formed when a diffusing molecule passes in the polymer matrix, the extended length of the diameter to diffuse is larger in the denser polymer matrix. The CED should increase because the molar volume of the polymer decreases with increasing density of the polymer. Therefore, the densification of the membrane, of course, in the BTDA–BAPP membrane, results in an increase in the activation energy for the diffusion. Moreover, this densification was caused by UV-irradiation in these membranes.

Dependencies of Permeability Coefficients and Gas Selectivities on Membrane Thickness

It was suggested from the ATR analysis that the membrane became chemically asymmetric. For the gas-permeation properties, the UV-irradiation made the membrane inhomogeneous. The apparent permeability coefficients for relatively large gas molecules remarkably depended on the membrane thickness. Figure 7 shows the relationship between the reciprocal of the permeability coefficients for H_2, O_2, N_2, and CO_2 and that of the membrane thickness. The apparent permeability coefficients for O_2 decreased with decreasing membrane thickness. This is due to the densification at the irradiated side of the membranes. In the apparent permeability coefficient for N_2 and CO_2, further dependence was found. In the O_2, N_2, and CO_2 permeation, the apparent permeability coefficients in the thicker membrane is larger than are those of the thinner one because the dense layer in the thicker one is thinner compared with the overall thickness and the effect of the dense layer is estimated to be small in the apparent permeability coefficient when the thicknesses of the dense layer in two membranes are the same. On the other hand, that of H_2 was constant. In the H_2 permeation, the effective densified layer is too thin compared to the overall membrane thickness to be estimated in the permeability coefficients. The permselectivity consequently increased with decreasing membrane thickness. These results seem to indicate that the layer effec-

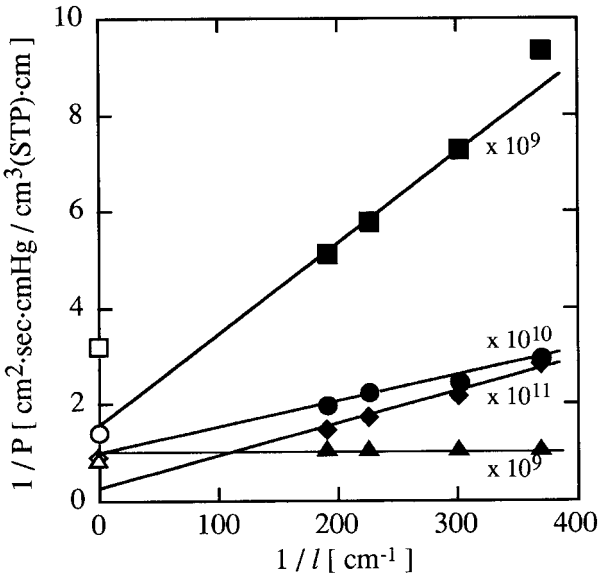

Figure 7 Relationship between the reciprocal of the permeability coefficients for (●) O_2, (♦) N_2, (▲) H_2, and (■) CO_2 at 50°C in the BTDA–BAPP membrane irradiated for 30 min and that of their thicknesses. Open symbols indicate $1/P$ in nonirradiated membrane.

tively densified by UV-irradiation is different for each penetrant molecule and that the membranes have become inhomogeneous in the direction for the gas permeation, and the above layer has the density distribution as schematically represented in Figure 8. In this figure, the blacker the color, the denser the membrane.

The reciprocal gas permeability coefficients in the nonirradiated membrane are also plotted on the infinite membrane thickness ($1/l = 0$) in Figure 7. The following equation can be derived from eq. (9) when $l_{1,2} \approx l_2$:

$$1/P_{1,2} = (l_1/P_1)(1/l_{1,2}) + 1/P_2 \qquad (15)$$

If it is assumed that the gas permeation through the UV-irradiated membranes can be treated with a simple binary layer, i.e., the effective densified layer and nonaffected layer, the intercept of the solid lines to the y-axis shows the reciprocal permeability coefficients in the nontreated layer. In H_2, the apparent permeability coefficients in the nonaffected layer, which were determined from the intercepts, were almost consistent with that of the nonirradiated membrane. This might indicate that there are no changes in the permeation properties for H_2 in the nonirradiated side of the membranes in the range of the studied membrane thickness. On the other hand, in O_2, N_2, and CO_2, the intercepts were derived from the permeability in the nonirradiated membrane and these derivations were toward the low permeabilities. These differences were larger as the diameter of the gas molecules were larger. This might also indicate that even at the nonirradiated side the membranes were effectively densified by the irradiation for the permeation of the large gas molecules as shown in Figure 8, and, then, in the range of the membrane thickness used in this study, it was not enough to meet the condition $l_{1,2} \approx l_2$.

Effect of Reannealing and UV-Irradiation

The apparent permeation properties in the membrane moderately cooled after the thermal imidization, one reannealed above T_g (240°C) and one reannealed followed by UV-irradiation, are listed in Table V. There were fewer effects of the reannealing on the permeabilities in the annealed membrane. Thus, the thermal treatment at the same temperature as that of the thermal imidization has less effect on the permeabilities. The thermal effect, such as lighting on the mercury lamp, on the gas permeabilities is, of course, negligible. However, the UV-irradiation caused the reannealed membrane to decrease in its permeabilities and efficiently increase the selectivity for H_2/N_2. These indicate that the UV-irradiation is quite an attractive method to increase the permselectivity compared to the thermal treatment.

The reductions in the permeabilities and increases in the permselectivities in the BTDA–BAPP membranes were due to the densification of the membranes, especially at the irradiated side, with UV-irradiation, resulting in the reduction in the diffusivity of the penetrants. It can be consid-

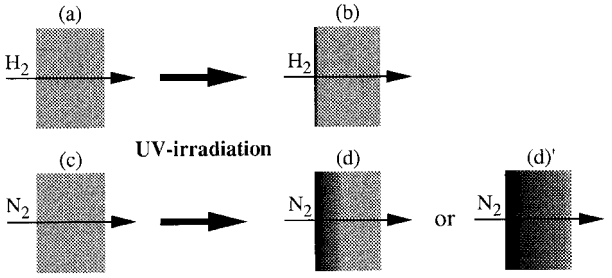

Figure 8 Schematic representations of the effective densified layer for the permeation of [(a), (b)] H_2 and N_2 [(c), (d), (d)′] gases in the UV-irradiated BTDA–BAPP membrane.

Table V Apparent Permeation Properties for the Gases Studied at 30°C in the BTDA–BAPP Membrane, One Reannealed Above T_g and One Reannealed Followed by UV-Irradiation

	$P_{app.}$[a]				$D_{app.}$[b]			$S_{app.}$[c]			
Condition	O_2	N_2	H_2	CO_2	O_2	N_2	CO_2	O_2	N_2	CO_2	PH_2/PN_2
Nontreated	0.45	0.060	7.7	2.3	0.96	0.19	0.17	4.7	3.1	138	130
Annealed	0.44	0.063	7.8	2.3	0.99	0.22	0.17	4.5	3.0	138	124
Annealed + UV[d]	0.36	0.046	7.0	1.8	0.75	0.14	0.12	4.8	3.4	144	152

[a] Apparent permeability coefficient $\times 10^{10}$ [cm^3 (STP) cm/cm^2 s cmHg].
[b] Apparent diffusion coefficient $\times 10^8$ (cm^2/s).
[c] Apparent solubility coefficient $\times 10^3$ [cm^3 (STP)/cm^3 (polymer) cmHg].
[d] Membrane annealed followed by 10 min UV-irradiation.

ered that these densifications are due to the following effects: (1) formation of intermolecular crosslinking, (2) increase in the polarity due to oxidation, (3) formation of the intermolecular charge-transfer complex, i.e., the well-known phenomenon concerning the polyimide materials as being thermally treated,[26,27] and (4) relaxation of the free volume that exists in the glassy polymers as the unrelaxed free volume, or that these occur simultaneously. Details will be discussed in the near future.

Gas-Sorption Property

Figure 9 shows the sorption isotherm for CO_2 in the successively UV-irradiated BTDA–BAPP and BTDA–BAPP(Q) polyimide, respectively, at 35°C. All isotherms are concave to the pressure axis in the range of the investigated pressure, which is characteristically found in the condensable gas sorption into glassy polymers. The dual-mode sorption parameters calculated by a nonlinear least squares using eq. (11) are listed in Table VI. In these parameters, C'_H, which is associated with the unrelaxed free volume in the glassy polymers, is sensitive to the glassy states of the polymers and one of the powerful tools to understand the morphologies of glassy polymers in characterizing their permeation properties. Although this parameter, C'_H, is also an apparent value because of being asymmetric with the irradiation, it seemed to be valid to compare it between the parameters in the specimens prepared from the same membrane having a constant thickness under the uniform condition. The C'_H of the nontreated BTDA–BAPP(Q) was larger than that of BTDA–BAPP, which was expected from the gas permeabilities in both membranes. It is well

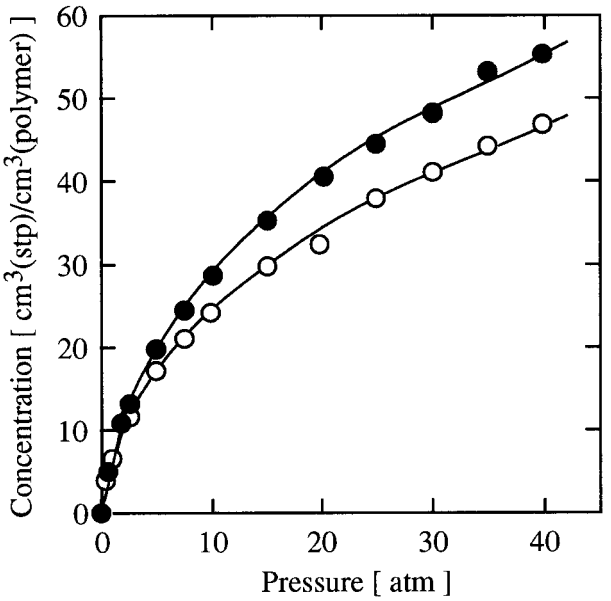

Figure 9 CO_2 sorption isotherm in the (○) BTDA–BAPP and (●) BTDA–BAPP(Q) membranes at 35°C.

Table VI Dual-mode Sorption Parameters for CO_2 at 35°C in the UV-Irradiated BTDA–BAPP and BTDA–BAPP(Q) Membranes

Membrane	Irradiation Time (min)	C'_H[a]	b[b]	k_D[c]
BTDA–BAPP	0	24.0	0.30	0.64
	10	25.5	0.25	0.61
	20	26.0	0.25	0.61
	30	27.5	0.24	0.61
BTDA–BAPP(Q)	0	33.3	0.20	0.66
	10	29.3	0.21	0.69
	30	29.9	0.19	0.66

[a] [cm^3 (STP)/cm^3 (polymer)].
[b] [atm^{-1}].
[c] [cm^3 (STP)/cm^3 (polymer) atm].

known that the C'_H of the quenched membrane is larger than that of one moderately cooled.[15] The UV-irradiation for 10 min on the quenched membrane, BTDA–BAPP(Q), decreased its C'_H. This phenomenon was observed in the same polyimide and the other one irradiated with a low-pressure mercury lamp as reported previously.[10] This decreasing in C'_H means a decreasing in the unrelaxed free volume, namely, the relaxation of the glassy polymer to an equilibrium state. On the other hand, in the moderately cooled BTDA–BAPP membrane, C'_H increased monotonically with increase in the UV-irradiation time. In general, the penetrants are more permeable through this volume with increasing C'_H. Except in the short-time irradiation on the BTDA–BAPP(Q), these increases are opposite to the results of the permeabilities. It is unclear why such phenomena have occurred with UV-irradiation and are being investigated now.

CONCLUSIONS

The permeabilities for the gases investigated in the polyimide membranes decreased with increasing UV-irradiation time. These decreases were remarkable for the large penetrants such as N_2 and CO_2. These were due to the decrease in the diffusivities of the penetrants by means of the densification by irradiation. This resulted in increasing the permselectivity for a gas pair with the different sizes, H_2 and N_2, without significant reduction in the flux for the more passage component, H_2.

The permeability coefficients and separation factors in the UV-irradiated membrane significantly depended on their thickness. These were due to that the membrane was asymmetrically densified by UV-irradiation and the thickness of the effective densified layer differed with respect to the penetrants.

The degree of the decreases in the permeabilities varied with the method of the UV-irradiation or cooling procedure after the thermal imidization. Especially, the relaxation of the glassy state with the short-time irradiation was observed in the quenched membrane. However, in all cases, the decreases in permeabilities were due to the densification of the membranes with the irradiation. UV-irradiation efficiently increased the gas selectivities for H_2/N_2 in the polyimide membrane studied even after reannealing above its T_g.

REFERENCES

1. T. H. Kim, W. J. Koros, G. R. Husk, and K. C. O'Brien, *J. Membr. Sci.,* **37,** 45 (1988).
2. K. Tanaka, H. Kita, M. Okano, and K. Okamoto, *Polymer,* **33,** 585 (1992).
3. S. A. Stern, Y. Liu, and W. A. Feld, *J. Polym. Sci. Part B Polym. Phys.,* **31,** 939 (1993).
4. M. Langsam and W. F. Burgoyne, *J. Polym. Sci. Part A Polym. Chem.,* **31,** 909 (1991).
5. G. F. Sykes and A. K. St. Clair, *J. Appl. Polym. Sci.,* **32,** 3725 (1986).
6. K. Matsumoto and P. Xu, *J. Membr. Sci.,* **81,** 23 (1993).
7. R. A. Hayes, U.S. Pat. 4,717,393 (Jan. 5, 1988). (to E. I. Du Pont de Nemours and Co.).
8. H. Kita, T. Inada, K. Tanaka, and K. Okamoto, *J. Membr. Sci.,* **87,** 139 (1994).
9. Y. Liu, M. Ding, and J. Xu, in *Proceedings of International Membrane Science and Technology Conference,* Nov. 10–12, 1992, Sydney, Australia, E2-7.
10. S. Matsui, T. Ishiguro, A. Higuchi, and T. Nakagawa, J. Polym. Sci. Part B Polym. Phys., **35,** 2259 (1997).
11. R. M. Barrer, *Trans. Faraday Soc.,* **35,** 628 (1939).
12. C. Rogers, V. Stannett, and M. Szwarc, *Ind. Eng. Chem.,* **49,** 1933 (1957).
13. R. M. Barrer, J. A. Barrie, and J. Slater, *J. Polym. Sci.,* **27,** 177 (1958).
14. A. S. Michaels, W. R. Vieth, and J. A. Barrie, *J. Appl. Phys.,* **34,** 1 (1963).
15. H. Hachisuka, Y. Tsujita, A. Takizawa, and T. Kinoshita, *J. Polym. Sci. Part B Polym. Phys.,* **29,** 11 (1991).
16. M. J. El-Hibri and D. R. Paul, *J. Appl. Polym. Sci.,* **30,** 3649 (1985).
17. H. Hachisuka, Y. Tsujita, A. Takizawa, and T. Kinoshita, *Polym. J.,* **21,** 1019 (1989).
18. J. S. Chiou and D. R. Paul, *J. Membr. Sci.,* **32,** 195 (1987).
19. D. S. Pope, G. K. Fleming, and W. J. Koros, *Macromolecules,* **23,** 2988 (1990).
20. N. J. Harrick, *J. Phys. Chem.,* **64,** 1110 (1960).
21. F. M. Mirabella, *J. Polym. Sci. Part B Polym. Phys.,* **21,** 2403 (1983).
22. C. Rogers, J. A. Meyer, V. Stannett, and M. Szwarc, *Tappi,* **39,** 737 (1956).
23. A. A. Lin, V. R. Sastri, G. Tesoro, A. Reiser, and R. Eachus, *Macromolecules,* **21,** 1165 (1988).
24. J. O. Hirschfelder, C. F. Curtiss, and R. B. Bird, *Molecular Theory of Gases and Liquids,* Wiley, New York, 1954.
25. P. Meares, *J. Am. Chem. Soc.,* **76,** 3415 (1954).
26. E. D. Wachsman and C. W. Frank, *Polymer,* **29,** 1191 (1988).
27. M. Hasegawa, I. Mita, M. Kochi, and R. Yokota, *J. Polym. Sci. Part C Polym. Lett.,* **27,** 263 (1989).